

Phase separation and magnetic structure in praseodymium disilicide

This article has been downloaded from IOPscience. Please scroll down to see the full text article.

1991 J. Phys.: Condens. Matter 3 3113

(<http://iopscience.iop.org/0953-8984/3/18/006>)

View [the table of contents for this issue](#), or go to the [journal homepage](#) for more

Download details:

IP Address: 171.66.16.147

The article was downloaded on 11/05/2010 at 12:05

Please note that [terms and conditions apply](#).

Phase separation and magnetic structure in praseodymium disilicide

B Lambert-Andron†, F Sayetat†, S Auffret‡, J Pierre‡ and R Madar§

† Laboratoire de Cristallographie, CNRS, 166 X, 38042 Grenoble Cédex, France

‡ Laboratoire L Néel, CNRS, 166 X, 38042 Grenoble Cédex, France

§ Institute National Polytechnique de Grenoble, Ecole Nationale Supérieure de Physique de Grenoble (Unité de Recherche associée au CNRS 1109) BP 46, 38042 Saint Martin d'Hères, France

Received 5 October 1990

Abstract. Praseodymium disilicide exhibits a phase separation near 200 K into two nearly tetragonal phases. The lattice parameters and the proportion of each phase are studied as functions of the temperature by x-ray and neutron diffraction; anomalous thermal expansion is observed for one of them. Both phases order magnetically at 12 K, with different magnetic structures.

1. Introduction

Rare-earth 'disilicides', which have been studied for over two decades, have recently attracted much interest when it has been demonstrated that they can be epitaxially grown on silicon. In spite of numerous crystallographic studies, some uncertainties still remain concerning their crystallographic superstructures and transformations. The present paper is devoted to the crystallographic and magnetic structures of praseodymium silicide PrSi_{2-x} .

X-ray diffraction investigations [1] established that the 'disilicides' of rare-earth metals RSi_{2-x} ($0 < x < 0.4$) crystallize either as the tetragonal ThSi_2 type, or as the orthorhombic GdSi_2 type, or with the hexagonal AlB_2 -type structure. Perri *et al* [2] observed a crystallographic transformation occurring near 150 K for PrSi_2 , and slightly above room temperature for NdSi_2 , from the tetragonal high-temperature phase to an orthorhombic form at low temperatures. Dijkman *et al* [3] investigated the temperature variation in lattice parameters in LaSi_2 , CeSi_2 and PrSi_2 compounds. By lowering the temperature, a crystallographic transformation starts at around 220 K for PrSi_2 . The room-temperature tetragonal phase transforms gradually and only partly into a low-temperature tetragonal structure with lower lattice parameters; the c -parameter of the starting phase increases anomalously during the transformation.

More recently, the binary phase diagram of Pr–Si has been investigated by Eremenko *et al* [4]. The congruent phase corresponds to a composition $\text{PrSi}_{1.8}$, with a rather broad homogeneity range. The high-temperature modification is the tetragonal phase, which transforms at 430 K for the Pr-rich boundary, and at 150 K for the Si-rich boundary

towards another structure. A similar structure transformation has been recently observed for $\text{CeSi}_{1.95}$ by Madar *et al* [5].

Houssay *et al* [6] give the homogeneity range of different phases, and the variation in the lattice parameters as a function of composition for several RSi_{2-x} compounds: PrSi_{2-x} compounds at room temperature are tetragonal from PrSi_2 to $\text{PrSi}_{1.75}$ and orthorhombic from $\text{PrSi}_{1.75}$ to $\text{PrSi}_{1.6}$.

Questions remain concerning the exact structure of the low-temperature phases, and their relation to the room-temperature tetragonal phase. In order to elucidate these points and to study the magnetic order in this system, we performed x-ray and neutron diffraction on polycrystalline samples of PrSi_{2-x} at the Si-rich boundary of the compound.

2. Sample preparation and experimental methods

The starting elements with atomic ratio 1:2 were melted in a water-cooled copper crucible under purified argon. The ingots were cooled at a rate of about 100 K min^{-1} .

X-ray experiments were performed using a high-resolution low-temperature diffractometer, using the $K\alpha_1$ radiation of chromium selected by a monochromator.

Neutron diffraction studies were performed at Institute Laue-Langevin using the D1B diffractometer. The incident wavelength was 2.525 \AA . Two powdered samples of praseodymium silicide prepared in the same manner were studied, in order to check the reproducibility of experimental results. It should be noted that the two samples had different thermal histories, as one was previously studied at low temperatures. Neutron diffraction allows us to refine the silicon concentration, as its scattering length is of the same order of magnitude as that of Pr.

X-ray patterns obtained at room temperature showed a slight excess of free silicon in addition to a tetragonal PrSi_{2-x} compound, with the lattice parameters $a = 4.205(5) \text{ \AA}$ and $c = 13.73(2) \text{ \AA}$. These data are in good agreement with previous data for PrSi_2 (ThSi_2 type; space group, $I4_1/amd$), but the true composition of the compound cannot be deduced precisely from the lattice parameters in the range $0 < x < 0.15$ [6].

The position parameter of Si and composition were refined from neutron diffraction results. The position parameters are

$$\text{Pr (4a site) } (0, 0, 0)$$

$$\text{Si (8e site) } (0, 0, z = 0.416)$$

and the composition is obtained as $\text{PrSi}_{1.95 \pm 0.05}$.

3. Low-temperature structure determination

3.1. X-ray studies

Scans were performed on the reflections (220), (109), (312) and (305), at different temperatures between 6 and 300 K. A broadening of the reflections, particularly (109), begins to arise at 210 K; the splitting of these reflections into two components can be

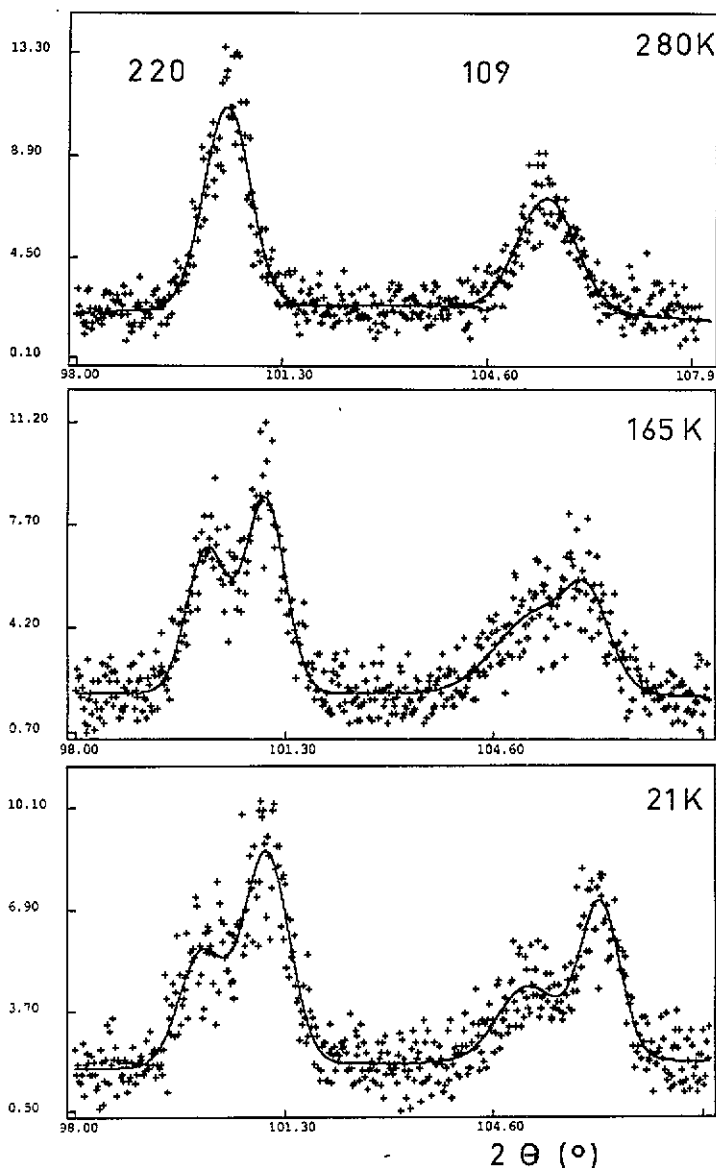


Figure 1. X-ray diffraction profiles of $[1, 0, 9]$ and $[2, 2, 0]$ reflections at various temperatures.

resolved below 190 K (figure 1). The relative intensities of the two components and the coherence of the parameter refinement shows that the larger c - and the larger a -parameters are associated in the same phase, in agreement with the analysis of Dijkman *et al* [3].

The (220) and (109) reflections are split into peaks with similar widths, while the (312) and (305) reflections are resolved into two peaks with unequal widths, the smaller-angle peak being broader. Thus it seems that the phase with the larger volume should be weakly distorted; however, this distortion cannot be measured with our experimental

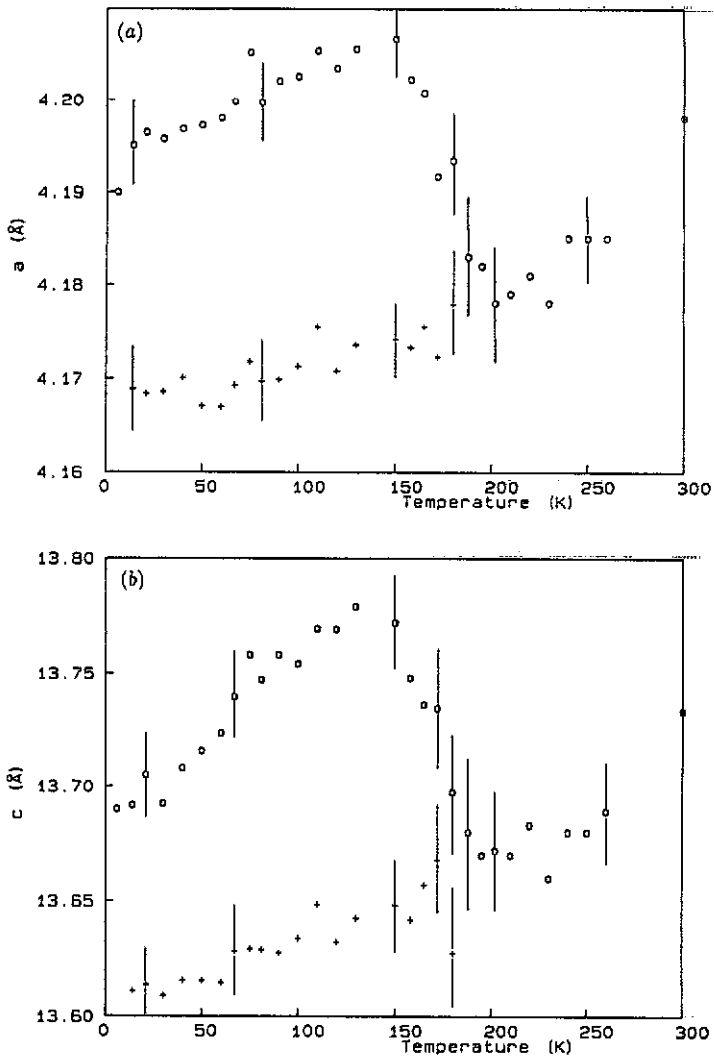


Figure 2. Lattice parameters (a) a and (b) c as a function of temperature .

resolution. On the assumption in a first approximation that the two phases are tetragonal, the thermal dependence of the lattice parameters for both phases is given in figure 2. It is readily seen that one of the phases (with the lower parameters) follows the usual Debye law, while the other phase undergoes a smooth transition in the 130–220 K temperature range. This transition is accompanied by a large increase in a and c . This behaviour may, however, be characteristic of a first-order transition, smeared out by inhomogeneities in the sample.

3.2. Neutron data

Several patterns were obtained for both samples between 1.22 K and room temperature, giving very similar results. Figure 3 represents all the spectra obtained for sample 1.

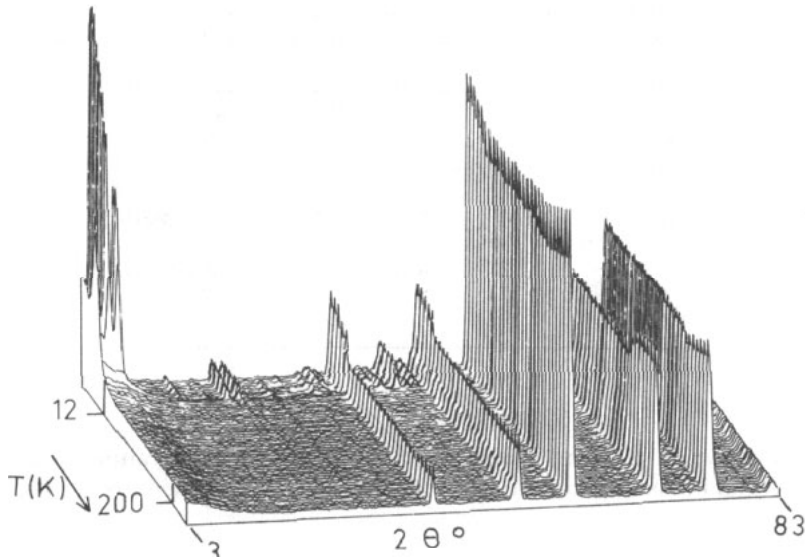


Figure 3. Neutron patterns of $\text{PrSi}_{1.95}$ as a function of temperature, showing the crystallographic transformation near 200 K and the onset of magnetic order at 12 K. (The temperature scale is not linear.)

Patterns taken from room temperature down to 180 K show a unique tetragonal phase with traces of silicon. The refinement of the structure gives a composition $\text{PrSi}_{1.95 \pm 0.05}$ (table 1) for both samples.

A splitting of the (105) reflection is observed for temperatures below 180 K. Apart from this splitting and a broadening of the (200) reflection, no other new reflection indicating some kind of superstructure appears on the patterns down to the magnetic ordering temperature (12 K). The poor resolution of the diffractometer at small scattering angles does not allow one to separate the lattice parameters of the two phases as precisely as in x-ray diffraction experiments.

3.3. Analysis of structural data

The observed phenomena are fully consistent with the data of Dijkman *et al* [3] for PrSi_2 , except that the phase separation occurs at present within a smaller temperature range. Two crystallographic phases coexist at low temperatures; in a first approximation, these phases can be considered as tetragonal, although a small orthorhombic distortion seems to be present at least in one phase. The respective proportions of the two phases remain constant below 100 K, being larger for the phase with the smaller c (73% of the whole for sample 1 and 76% for sample 2).

A surprising feature, already emphasized by Dijkman *et al*, is the fact that the phase with the larger c is the dominant phase just below the phase separation, the proportion of this phase decreasing at lower temperatures (the relative variation in the intensities for some reflections is shown in figure 1). Thus it looks as if the room-temperature tetragonal phase progressively disappears to be replaced by another phase of smaller

Table 1. Calculated and observed nuclear intensities for $\text{PrSi}_{1.95}$ at $T = 290$ K (corrected for the Lorentz factor). This refinement corresponds to the composition $\text{PrSi}_{1.95 \pm 0.05}$. p is the multiplicity.

h	k	l	p	I_{calc} (b)	I_{obs} (b)
1	0	1	8	3.84	3.85 ± 0.20
0	0	4	2	0.06	Not obtained
1	0	3	8	12.7	13.0 ± 1.5
1	1	2	8	85.6	85 ± 5.0
1	0	5	8	78.0	70 ± 11
2	0	0	4	90.7	99 ± 11

volume, while its own volume has an anomalous temperature variation. The same behaviour has been shown to occur for $\text{CeSi}_{1.86}$ [5]. These features will be analysed later.

4. Magnetic measurements and magnetic structure

4.1. Magnetization measurements

The magnetization and the initial susceptibility were measured on a $\text{PrSi}_{1.9}$ single crystal obtained by the Czochralski method. Measurements were performed from 1.5 to 300 K in a supraconducting coil in fields up to 7.5 T and these results have already been published [7]. The susceptibility is larger for a field applied perpendicular to the c axis than for a field along c . It follows that above 50 K a Curie–Weiss law holds along both directions, defining the Curie–Weiss parameters $\Theta_p^{\parallel c} = -8$ K and $\Theta_p^{\perp c} = +15$ K. The susceptibility perpendicular to c diverges at the Curie temperature $T_c = 12$ K. Below this temperature, the magnetization reaches saturation in two steps (figure 4), the saturation value being $1.8\mu_B$ at 1.5 K.

For a field parallel to c , the magnetization is much smaller than for H perpendicular to c , indicating that moments are confined in the planes perpendicular to the c axis.

4.2. Neutron diffraction and magnetic structure

Below 12 K, magnetic reflections appear on neutron patterns which are related to three inequivalent propagation vectors (figure 5). (The same patterns appear for the two different samples.)

First, the intensity of nuclear peaks increases, corresponding to a ferromagnetic component: $Q_0 = (0, 0, 0)$. Secondly, two satellites appear at small scattering angles, which belong to two different propagation vectors Q_1 and Q_2 . Many other satellites related to Q_1 and Q_2 occur throughout the diffraction pattern. We observe for instance two satellites $(0, 0, 2 \pm Q_1)$, four satellites related to Q_1 around $(1, 0, 1)$, two satellites related to Q_2 around $(1, 0, 1)$, etc. The indexation of these satellites allows one to determine the propagation vectors as $Q_1 = (0.094, 0.094, 0.067)$ and $Q_2 = (0.13, 0.13, 0)$. In addition, we may attribute the vector Q_0 to the phase with the smaller c , and the vector Q_1 to the phase with the larger c (location of $0, 0, 2 \pm Q_1$ satellites).

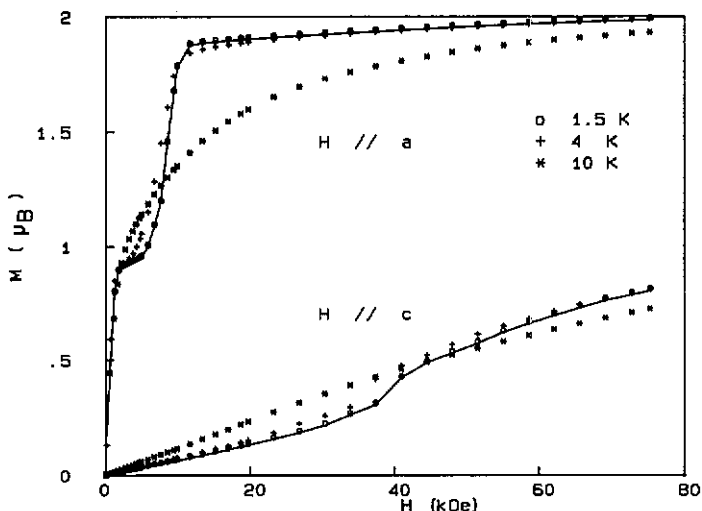


Figure 4. Magnetization of a PrSi_9 single crystal for a field along the a or c axis.

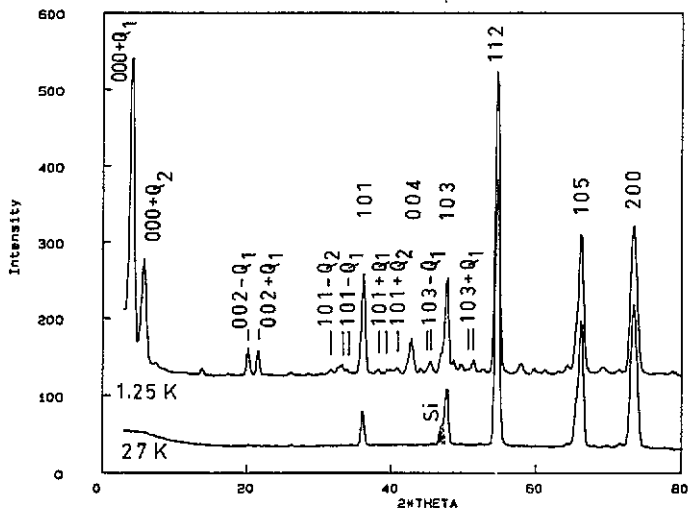


Figure 5. Neutron patterns at 1.25 and 27 K. Only the most important magnetic satellites have been indexed.

The case of the vector \mathbf{Q}_2 is more uncertain, but the location of $(1, 0, 1 \pm \mathbf{Q}_2)$ satellites is more consistent with the association of \mathbf{Q}_2 with the phase of smaller volume.

Figure 6 represents the thermal variations in intensities for the reflections $(1, 0, 1)_{\text{Ferro}}$, $(0, 0, 0 + \mathbf{Q}_1)$, and $(0, 0, 0 + \mathbf{Q}_2)$.

Within experimental precision, the components corresponding to the three propagation vectors appear at the same temperature (about 12 K). The intensity of the reflections $(0, 0, 0 + \mathbf{Q}_1)$ and $(1, 0, 1)_{\text{Ferro}}$ increases continuously with decreasing temperature, while that of $(0, 0, 0 + \mathbf{Q}_2)$ passes through a maximum at 8.5 K and decreases below this temperature.

The magnetic structures associated to each propagation vector were refined using the MXD program of Wolfers [8].

The Pr atoms in the crystallographic cell are described as follows:

atom	X	Y	Z
Pr(1)	0	0	$\frac{1}{2}$
Pr(2)	0	$\frac{1}{2}$	$\frac{1}{4}$
Pr(3)	$\frac{1}{2}$	$\frac{1}{2}$	$\frac{1}{2}$
Pr(4)	$\frac{1}{2}$	0	$\frac{3}{4}$

Experimental and calculated intensities corrected for the Lorentz factor are reported in tables 2–4. The ferromagnetic component associated with Q_0 is perpendicular to the c axis. The weighted reliability factor R is 6%. Taking into account the proportion of the crystallographic phase in the sample (about 75%), the magnitude of the moment is $(2.36 \pm 0.20)\mu_B$ in the first sample, and $(2.45 \pm 0.25)\mu_B$ for the second sample.

The magnetic structure associated with Q_1 has two components parallel to the x and y axes. The different arrangements of the four moments of the crystallographic cell can be described by several modes, for instance $F \equiv (++++)$ is the mode with all parallel spins, $A \equiv (+-+-)$ is a mode where the direction of spins alternate, etc. In addition, different modes can apply to the different components of spins. In the present case, the best fit is obtained for the model corresponding to the arrangements A for the x component and F for the y component, giving a mode $A_x F_y$. Taking into account the proportion of the phase, $M_x = 1.4\mu_B$ and $M_y = 1.96\mu_B$. The magnitude of the resultant is $(2.40 \pm 0.2)\mu_B$, with $R = 8\%$.

The magnetic structure associated with Q_2 is described by a ferromagnetic arrangement F_x (or equivalently F_y) of the four basis moments, with $R = 15\%$.

It seems more plausible to associate the propagation vector Q_2 with the vector Q_0 in the crystallographic phase with the smaller c . Within this assumption, the magnitude of the Q_2 -component is obtained as $(0.65 \pm 0.15)\mu_B$, which gives a maximum resultant magnitude of $2.5\mu_B$ for the magnetic moment of this phase (and a small amplitude modulation), assuming that the two components are orthogonal. In the other case (Q_1 associated with Q_2), the magnetic structure would be extremely complicated, with a strong modulation of the magnitude of the moment.

The occurrence of two different magnetic structures helps one to understand the peculiar behaviour of magnetization for a field applied in the basal plane; the ferromagnetic component of one phase saturates in a low magnetic field, whereas a metamagnetic behaviour occurs for the second phase in a field of about 1 T.

Single-crystal diffraction studies can give precise information concerning the propagation vectors of the structure. Therefore, neutron Laue patterns were recently obtained for a $\text{PrSi}_{1.9}$ single crystal used for magnetic measurements. The instrument S42 of the Institute Laue-Langevin was used, with a low-temperature cryostat. Either the c axis or an a axis was oriented parallel to the neutron beam. In addition to the characteristic patterns from nuclear diffraction of the tetragonal structure, new sets of weak magnetic reflections appears below 12 K at small scattering angles. The analysis of these reflections

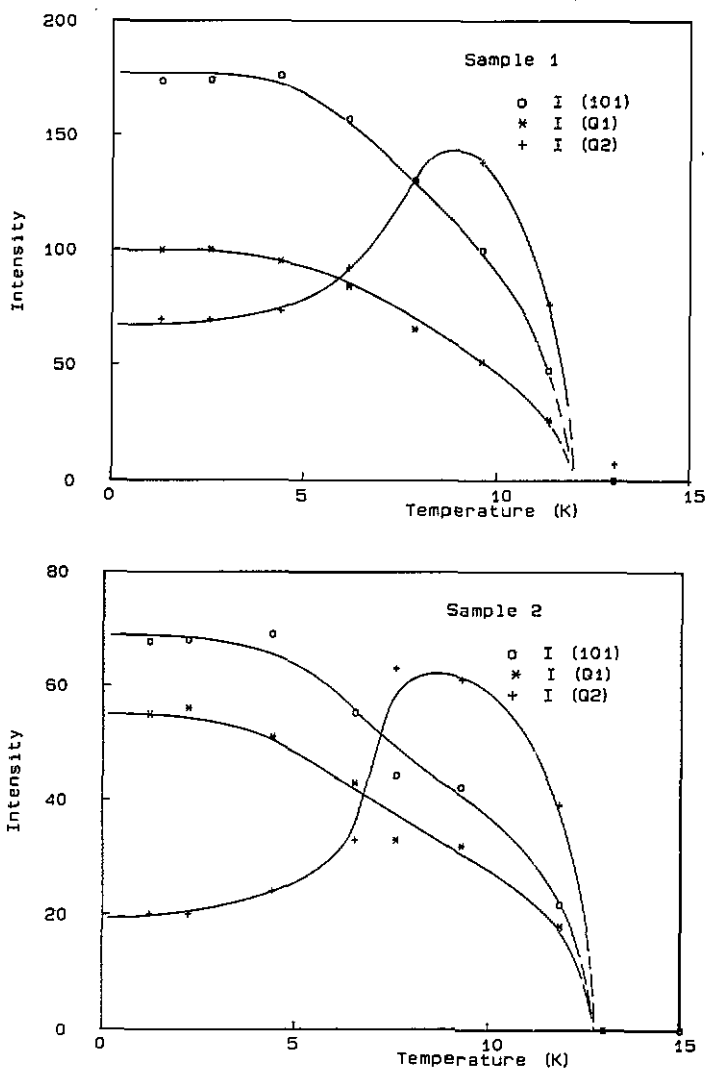


Figure 6. Temperature variation in the intensities of magnetic reflections for the two samples (corrected for Lorentz factor). $I(Q_1)$ is the intensity of the $[0, 0, 0, +Q_1]$ reflection; $I(Q_2)$ is the intensity of the $[0, 0, 0 + Q_2]$ reflection; $I[101]$ is the magnetic contribution to the $[101]$ reflection (divided by a factor of 10).

Table 2. Calculated and observed nuclear and ferromagnetic intensities for $\text{PrSi}_{1.95}$ at $T = 1.24$ K, corresponding to the configuration $F_x (M_{1x} + M_{2x} + M_{3x} + M_{4x})$, with $Q_0 = (0, 0, 0)$ and a value of the moment $M_x = (2.40 \pm 0.20)\mu_B$ in the major phase (see text).

h	k	l	I_{calc} (b)	I_{obs} (b)
1	0	1	14.2	15.3 ± 1.0
0	0	4	9.28	8.2 ± 1.2
1	0	3	25.5	23.7 ± 3.0
1	1	2	107	119 ± 20
1	0	5	91.0	77 ± 20

Table 3. Calculated and observed magnetic intensities for PrSi_{1.95} at $T = 1.24$ K, corresponding to the configuration $A_x (M_{1x} - M_{2x} + M_{3x} - M_{4x})$, $F_y (M_{1y} + M_{2y} + M_{3y} + M_{4y})$, with $Q_1 = (0.094, 0.094, 0.067)$ and a value of the moment equal to $(2.40 \pm 0.2)\mu_B$ in the minor phase.

h	k	l		I_{calc} (b)	I_{obs} (b)
0	0	0	$+Q_1$	1.13	1.15 ± 0.06
0	0	1	$-Q_1$	0	Not obtained
0	0	1	$+Q_1$	0	Not obtained
0	0	2	$-Q_1$	1.08	1.11 ± 0.12
0	0	2	$+Q_1$	1.08	1.09 ± 0.12
1	0	1	$-Q_1$	3.49	$2.7 \pm 1.0^*$
1	0	1	$+Q_1$	3.30	$2.2 \pm 1.5^*$

* Sum of two inequivalent satellites.

Table 4. Calculated and observed magnetic intensities for PrSi_{1.95} at $T = 1.24$ K, corresponding to the configuration $F_x (M_{1x} + M_{2x} + M_{3x} + M_{4x})$, with $Q_2 = (0.13, 0.13, 0)$ and a value of $M_x = (0.65 \pm 0.15)\mu_B$ in the major phase.

h	k	l		I_{calc} (b)	I_{obs} (b)
0	0	0	$+Q_2$	0.372	0.37 ± 0.03
0	0	2	$-Q_2$	0	Not obtained
0	0	2	$+Q_2$	0	Not obtained
1	0	1	$-Q_2$	0.802	0.60 ± 0.30
1	0	1	$+Q_2$	0.739	1.10 ± 0.50

is under way but is not straightforward, as different wavelengths contribute to the Laue patterns.

5. Discussion

The preceding diffraction results are supported by a study of the resistivity of polycrystalline PrSi₂ [9] (figure 7). In addition to the rapid decrease in the resistivity below 12 K due to magnetic order, the resistivity decreases anomalously below 160 K when the temperature is decreased and presents a strong irreversibility in this temperature range. The phenomena are even more pronounced than those observed for CeSi_{1.86} [5], where only a small resistivity anomaly was observed at the crystallographic transformation.

The present study confirms the results previously obtained by Dijkman *et al* for PrSi₂. The room-temperature tetragonal phase transforms partly at low temperatures to another phase, while its lattice parameters have an anomalous temperature variation. A striking feature is that the relative proportions of the two phases at low temperatures

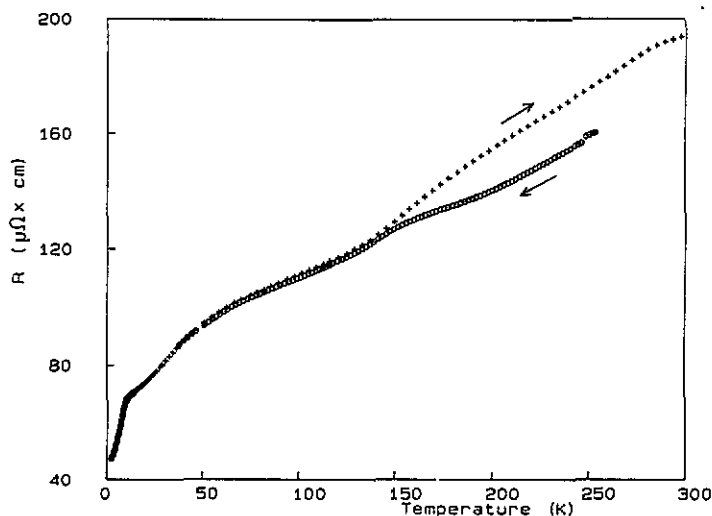


Figure 7. Resistivity for a PrSi_2 polycrystal starting a temperature cycle from room temperature in a virgin sample.

are rather independent of the sample and of its thermal history, ranging from 24–76% to 30–70% in the sample used by Dijkman *et al.* This indicates that we have to deal with a separation of two phases in equilibrium rather than to a simple incomplete phase transformation, and that the proportion of the phases is determined by the thermodynamics of the system rather than by its kinetics (cooling rate).

It seems that some kind of ordering of silicon vacancies occurs at least for one phase. Such an ordering has been evidenced for $\text{CeSi}_{1.86}$ [5] where a long-range superstructure has been observed by electron diffraction at low temperatures. The more rapid decrease in the electrical resistivity for PrSi_2 below 160 K (figure 7) also means reduced disorder scattering, which in the present case is too sudden to be explained by crystal-field effects. It is thus logical to assume that at least the low-temperature major phase (with smaller volume) is ordered. Cycling the temperature leads to an irreversibility of the resistivity variation, as if defects or phase separation effects were not cured when the temperature rises to 300 K.

A question remains of whether or not the phase separation is accompanied by a change in the silicon concentration, which is predicted by Gibbs' rule of phase equilibrium and would be particularly the case for spinodal decomposition. Owing to the number of independent parameters in the structure refinements, and the high correlation between them, it was not possible to obtain the composition for the two phases at low temperatures, which remains an important challenge.

In the present case, the compound is at the rich end of the homogeneity range, being in equilibrium with silicon at high temperatures. It is thus difficult to imagine a further large variation in the composition for the phase which would accept more silicon at low temperatures.

It is also difficult to deduce information about the Si concentration from the value of the lattice parameters; even at room temperature, the variation in c is not a monotonic function of Si concentration [6], the thermal expansion of different phases is not known and seems anomalous, at least for CeSi_{2-x} and PrSi_{2-x} compounds [3]. For instance, we

observe that the maximum values of the lattice parameters reach $a = 4.205(4) \text{ \AA}$ and $c = 13.78(4) \text{ \AA}$ at 130 K, values in perfect agreement with those reported by Dijkman *et al* (4.21 \AA and 13.78 \AA , respectively, between 130 and 150 K). Such a high value for c is only encountered at room temperature for the orthorhombic compound $\text{PrSi}_{1.6}$ ($a = 4.165 \text{ \AA}$, $b = 4.116 \text{ \AA}$ and $c = 13.81 \text{ \AA}$), but associated with a and b much smaller than observed. On the other hand, we cannot exclude the possibility that a true stoichiometric PrSi_2 phase exists at low temperatures, but again the volume would be larger than that of the room-temperature, most Si-rich phase ($a = 4.205 \text{ \AA}$ and $c = 13.73 \text{ \AA}$).

The magnetic study shows two different magnetic structures belonging to the two different phases. The moments for these structures are perpendicular to the c axis. The direction of the moments in the basal plane may give some information on the magnetocrystalline anisotropy in this plane. For instance, the ferromagnetic structure of pure heavy rare-earth metals is stabilized, compared with the helimagnetic structure, by a lowering of the hexagonal symmetry due to magnetostriction. Similarly, the (nearly) ferromagnetic phase of $\text{PrSi}_{1.9}$ (with lower c) may be stabilized by the particular arrangement of silicon vacancies in this phase, giving a large magnetocrystalline anisotropy in the basal plane. Conversely, the modulated magnetic structure of the other phase could be related to a modulated order of silicon vacancies.

Acknowledgments

We thank J L Soubeyrou for his kind help during the neutron diffraction experiments, J Cl Marmeggi for the neutron Laue experiments and E Siaud for preparing the samples.

References

- [1] Iandelli A and Palenzona A 1978 *Handbook on the Physics and Chemistry of Rare Earths* vol 2, ed K A Gschneidner and L R Eyring (Amsterdam: North-Holland) p 1
Rogl P 1978 *Handbook on the Physics and Chemistry of Rare Earths* vol 7, ed K A Gschneidner and L R Eyring (Amsterdam: North-Holland) p 51
- [2] Perri J A, Banks E and Post B 1959 *J. Phys. Chem.* **63** 2073
- [3] Dijkman W H, Moleman A C, Kessler E, de Boer F R and de Châtel P F 1982 *Valence Instabilities* ed P Wachter and H Boppart (Amsterdam: North-Holland) p 515
Dijkman W H 1982 *Thesis* University of Amsterdam
- [4] Eremente V N, Meleshevich K A and Buyanov Y I 1986 *Izv. VUZ Tsvetn. Metall.* **3** 82-7
- [5] Madar R, Lambert B, Houssay E, Meneau d'Anterroches C, Pierre J, Laborde O, Soubeyrou J L, Rouault A, Pelissier J and Sénateur J P 1990 *J. Mater. Res.* **5** 2126-32
- [6] Houssay E, Rouault A, Thomas O, Madar R and Sénateur J P 1989 *Appl. Surf. Sci.* **38** 156-61
- [7] Pierre J, Auffret S, Siaud E, Madar R, Houssay E, Rouault A and Sénateur J P 1990 *J. Magn. Magn. Mater.* **89** 86-96
- [8] Wolfers P 1990 *J. Appl. Crystallogr.* at press
- [9] Pierre J, Siaud E and Frachon D 1988 *J. Less-Common Met.* **139** 321-9